A NEW LOW-TURBULENCE WIND TUNNEL FOR BIRD FLIGHT EXPERIMENTS AT LUND UNIVERSITY, SWEDEN

C. J. PENNYCUICK[1],[*], THOMAS ALERSTAM[2] AND ANDERS HEDENSTRÖM[2]

[1]*School of Biological Sciences, University of Bristol, Woodland Road, Bristol BS8 1UG, UK* and [2]*Department of Animal Ecology, Lund University, Ecology Building, S-223 62 Lund, Sweden*

Summary

A new wind tunnel for experiments on bird flight was completed at Lund University, Sweden, in September 1994. It is a closed-circuit design, with a settling section containing five screens and a contraction ratio of 12.25. The test section is octagonal, 1.20 m wide by 1.08 m high. The first 1.2 m of its length is enclosed by acrylic walls, and the last 0.5 m is open, giving unrestricted access. Experiments can be carried out in both the open and closed parts, and comparison between them can potentially be used to measure the lift effect correction. The fan is driven by an a.c. motor with a variable-frequency power supply, allowing the wind speed to be varied continuously from 0 to 38 m s^{-1}. The whole machine can be tilted to give up to 8 ° descent and 6 ° climb. A pitot-static survey in the test section showed that the air speed was within ±1.3 % of the mean at 116 out of 119 sample points, exceeding this deviation at only three points at the edges. A hot-wire anemometer survey showed that the turbulence level in the closed part of the test section was below 0.04 % of the wind speed throughout most of the closed part of the test section, rising to approximately 0.06 % in the middle of the open part. No residual rotation from the fan could be detected in the test section. No decrease in wind speed was detectable beyond 3 cm from the side walls of the closed part, and turbulence was minimal beyond 10 cm from the walls. The installation of a safety net at the entrance to the test section increased the turbulence level by a factor of at least 30, to 1.2 % longitudinally and 1.0 % transversely.

Key words: wind tunnel, bird, flight, low turbulence.

Introduction

Principle of wind tunnel experiments

It appears that Greenewalt (1961) was the first to apply the principle of the wind tunnel to the study of bird flight, by placing a hummingbird feeder directly downstream of an electric fan. He was able to control the bird's air speed by adjusting the speed of the fan, while maintaining its ground speed at zero. This enabled him to make measurements of wing kinematics from film in which the bird remained stationary relative to the camera. Zero ground speed is not the same as 'hovering', which means flight at zero air speed. The bird's exertions depend on its air speed, not its ground speed, and these two speeds are only the same if the wind speed is zero. If the wind speed in the wind tunnel is uniform, and the turbulence level is low, then flight at zero ground speed is mechanically and physiologically the same as flight through still air, at an air speed equal and opposite to the wind speed. The difference from the free-flight situation is that the bird's air speed can be determined and held constant by the experimenter. If the wind tunnel can be tilted, the angle of climb or descent is also under the experimenter's control.

While it is not difficult to generate a flow of wind in which a bird can fly, it is another matter altogether to do so in a manner that will permit such quantities as fuel consumption, optimum flight speeds and so on to be reliably measured. Since the 1960s, a number of small wind tunnels have been built especially for bird flight experiments, all of which have been subject to serious design compromises imposed by space restrictions and limited funds. We initiated a design study in 1991, from which we concluded that any major advance in wind tunnel studies on birds would require a much larger machine than any currently in service. We explain below the principles underlying our design, then we describe the main constructional features of the Lund wind tunnel and present the results of performance tests.

Specification

Basic design requirements

Bird experiments usually depend on training a bird to fly in the test section, without any physical restraint, rather than on

*e-mail: C.Pennycuick@bristol.ac.uk.

mounting a model on a balance, as is usual in engineering wind tunnels. Our specification did not include any provision for balances, but it did call for two features which are not normally found in engineering wind tunnels: (1) easy access to the test section during experiments; and (2) provision for tilting the whole machine, so that the air stream can be inclined to the horizontal. We required a test section at least 1 m wide and a continuously variable wind speed from 0 to at least $30\,\mathrm{m\,s^{-1}}$. In the final design, these figures were revised upwards to 1.2 m and $38\,\mathrm{m\,s^{-1}}$.

Turbulence

The main distinguishing feature of this wind tunnel is that it was designed to produce a very low level of turbulence in the test section. This is a requirement to which we feel that insufficient attention has been given in previous wind tunnels designed for bird experiments. In model aircraft, which operate at similar scales (Reynolds numbers) to birds, massive differences of performance can result, depending on the extent to which the boundary layer is attached to the wing or body surface, and this in turn can be strongly affected by millimetre-scale turbulence in the air stream (Schmitz, 1960; Simons, 1994). Performance measurements made on a model in a wind tunnel with turbulence can give a highly misleading impression of the performance of the same model in free air, which normally does not contain turbulence on a scale that would directly affect the boundary layer. It is not known whether measurements on birds in wind tunnels with turbulence are subject to similar errors, but it seems likely that they would be. Such errors might be large and would apply to performance estimates of any kind, whether they are derived from physiological measurements of total fuel consumption or from more direct observations. We set out to create an air stream in which the level of small-scale turbulence is as low as possible, so as to give us the opportunity to investigate the behaviour of boundary layers over feathered surfaces, a subject about which nothing is known at present and which cannot be investigated in existing wind tunnels.
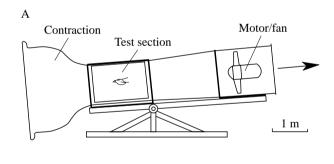
Contraction ratio

The requirements for producing low turbulence are well known (Pankhurst and Holder, 1965; Rae and Pope, 1984) and depend on accelerating the air in a 'contraction', that is a section with diminishing cross-sectional area, immediately upstream of the test section. Upstream of the contraction, velocity variations are evened out by wire mesh screens in a 'settling section', where the air speed is lower than in the test section, because the cross-sectional area is wider. The screens also serve to break large vortices into smaller eddies, which decay more quickly. The most important feature for minimising the turbulence level is the 'contraction ratio', that is, the ratio of the cross-sectional areas at the wide and narrow ends of the contraction. The flow velocity in the settling section is lower than that in the test section by a factor equal to the contraction ratio. The greater the contraction ratio, the lower the speed in the settling section, and the less the power needed

to drive the air through the screens, so that more screens can be used, making the eventual flow smoother. The contraction itself further reduces the turbulence in terms of percentage of the wind speed, since the wind speed increases by a factor equal to the contraction ratio, while the eddies are simply carried along, without any increase in their local velocities. The consensus among engineers is that a contraction ratio of 12 or greater is necessary to bring the root-mean-square (RMS) value of velocity fluctuations in the test section to below 0.05 % of the wind speed, which would be regarded as an acceptable criterion of 'low turbulence'.

Choice of layout

Most small, low-speed wind tunnels are of 'open-circuit' layout, in which air is sucked in at one end of the machine and blown out at the other. There are two kinds of open-circuit wind tunnels, the 'suction' type and the 'blower' type. The principle of the suction type is illustrated by Fig. 1A, which is based on an early suction wind tunnel, still in use at Duke University (Tucker and Parrott, 1970). The contraction ratio of this wind tunnel is approximately 4 (diameter ratio 2), which means that the wind speed increases by a factor of 4 as the air passes from the entrance of the contraction to the entrance of the test section. This acceleration is produced by a pressure gradient in the direction of the flow. As the air is at ambient pressure at the entrance to the contraction, it must be below ambient in the test section, hence the term 'suction'. This type
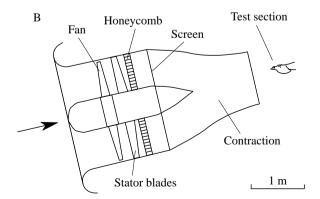

Fig. 1. The two generic types of open-circuit wind tunnel. (A) Suction tunnel, after Tucker and Parrott (1970). (B) Blower tunnel, after Pennycuick (1968). The direction of air movement is shown by the arrows.
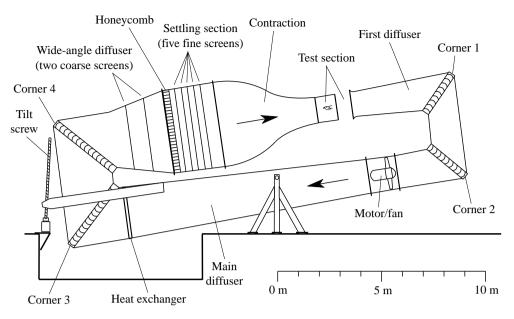
Fig. 2. Layout of the Lund wind tunnel. The direction of air movement is shown by the arrows.

of wind tunnel only works properly if the test section is carefully sealed, otherwise air rushes in through any gaps or holes and disrupts the flow in the test section. Although this is usually not a problem in engineering applications, it is difficult to control a free-flying bird in a test section that is closed and sealed. In practice, experimenters tend to work with the door open and to make holes for wires and tubes, which unfortunately modifies the flow in ways that cannot be quantified. Some other well-known wind tunnels have used the open-circuit suction plan, notably the one at Saarbrücken, Germany, of which technical details and drawings were given by Rothe and Nachtigall (1987). This wind tunnel also has a contraction ratio of 4, with a 1 m×1 m cross section, 1.4 m long. It is not tiltable, but it has an upstream settling section with four screens to smooth out the flow. Good success has been achieved with training pigeons and other birds to fly in this wind tunnel, in spite of the difficulty of access to the test section. Nachtigall (1995) has reviewed the extensive series of experiments, mostly physiological in character, which have been carried out with it.

In the blower type of open-circuit wind tunnel, the fan is upstream, and pressure is equal to ambient at the exit. The 'test section' can simply be the open space outside the end of the contraction, but precautions are necessary to smooth out the disturbance caused by the fan. Fig. 1B shows a blower design from Pennycuick (1968), with stator vanes designed to remove the rotation caused by the fan, then a metal honeycomb to align the flow with the tunnel axis, and a fine wire-mesh screen at the entrance to the contraction. This layout allowed unrestricted access to the bird, at the expense of some unevenness and turbulence of the flow caused by the upstream fan. These effects could have been reduced if the settling section had been longer, with more screens, and if the contraction ratio (also approximately 4) had been greater, but limitations of space and funds precluded this.

Our eventual contraction ratio of 12.25 in the present wind tunnel results in a settling section 4 m across, which is inconveniently large for any kind of open-circuit design. We opted instead for the 'up-and-over' closed-circuit layout shown diagrammatically in Fig. 2. The design was adapted from an existing low-turbulence wind tunnel at the Department of Aerospace Engineering at the University of Bristol, designed and described by Barrett (1984). The contraction and test sections are on the upper level, and the motor and fan are in the return path below. Detailed engineering drawings and cost estimates were prepared from our preliminary design by AB Rollab of Solna, Sweden, and this firm was subsequently appointed the main contractor for the construction of the wind tunnel at Lund University. Rosén and Nyström (1997) have described the design and construction of the wind tunnel from the engineering standpoint. The main characteristics of the final design are summarised in Table 1.

Main features of the Lund wind tunnel
Test section

We now briefly explain the functions of the main components, beginning with the test section, and following the air flow around the circuit. Our specification called for unrestricted access to a bird flying in the test section, meaning that the tunnel has to be designed in such a way that the pressure in the test section is equal to the ambient pressure outside. This is achieved by having an opening at the test section, while the rest of the circuit is sealed. As the test section is the narrowest part of the circuit, it is also the part where the air velocity is highest and, therefore, by Bernoulli's principle, where the pressure is lowest. Everywhere else in the circuit, the pressure is higher than ambient, reaching a maximum in the settling section, upstream of the contraction. For the first 1.2 m of its length, the test section is enclosed by acrylic walls, but there is then a 0.5 m gap for pressure equalisation, before the bell-mouth entry to the first diffuser. The height of the

Layout: vertical recirculating, test section above, motor below
Contraction ratio: 12.25
Screens: five
Test section: octagonal. Width 1.20 m at the upstream end, increasing to 1.22 m at the end of the closed section. Height constant at 1.08 m. Length of closed section 1.2 m, open section 0.5 m
Recommended maximum bird wing span: 0.80 m
Motor and fan: 440 V three-phase, by ABB of Finland, driving 10-bladed Novenco fan of 1.6 m diameter. Solid-state, variable-frequency power supply delivers 27 kW at 50 Hz (maximum) at a fan speed of 961 revs min^{-1}
Wind speed: continuously variable from 0 to 38 m s^{-1}
Turbulence level: below 0.04 % at 10 m s^{-1}
Tilt: +8 ° (descent) to −6 ° (climb)
Temperature: cooler capable of maintaining −5 °C coolant temperature. Air temperature depends on wind speed and ambient temperature

closed part of the test section is 1.08 m, and its width is 1.20 m at the upstream end and 1.22 m at the downstream end. This widening is intended to compensate for the increasing thickness of the boundary layer along the wall, and does not represent an increase in the usable width of the test section.

The gap is an essential feature of the design and is a part of the test section, which can be used for experiments. In effect we have a dual test section, with a closed part for the first 1.2 m and an open part for the remaining 0.5 m. We hope to exploit this feature to measure the 'lift effect', one of the sources of error inherent in wind tunnel measurements. A theoretical treatment of this effect for fixed wings is given in Pankhurst and Holder (1965) and Rae and Pope (1984), but it is not possible to estimate it reliably for flapping wings. In a closed test section, the air speeds up a little as it squeezes between the wing and the walls, which has the effect of making the measured lift:drag ratio higher than it would be in free air. According to theory, the boundary of an open jet also produces an error of the same magnitude, but in the opposite direction; that is, it decreases the measured lift:drag ratio. Thus, if the same measurement can be carried out first in the closed part of the test section and then repeated in the open part, the mean of the two observations should be a good estimate of the 'free-air' result, while the difference between them should be equal to twice the magnitude of the error.

The lift effect is one of several well-known effects whereby the proximity of a solid wall or an open-flow boundary modifies the flow around an object in the test section (Pankhurst and Holder, 1965; Rae and Pope, 1984). These effects may cause errors in measurements on birds flying in the wind tunnel, regardless of whether the measurements are made by mechanical or physiological methods. To keep the magnitude of any such errors small, it is best to keep well clear of the walls. As a practical rule, the wing span of a bird flying in any wind tunnel should not exceed two-thirds of the width of the test section.

First diffuser to fan

At the downstream end of the test section, the air is collected by a bellmouth and enters a short diverging section, the 'first diffuser', in which the speed decreases and the pressure increases by a small amount. This is followed by the first and second corners, each consisting of a vertical right-angled bend in the tunnel, with an array of curved steel vanes to guide the air around each corner. The cross-sectional area is constant throughout this section, which serves to take the air flow to the lower level, turn it through 180 ° and deliver it to the fan, without any change of speed or pressure. Power for the tunnel comes from a three-phase a.c. motor from Asea Brown Boveri (ABB) of Finland, driving a 10-bladed Novenco fan of 1.60 m diameter, mounted in a cylindrical steel casing. To minimise noise and vibration, the casing is supported on rubber shock mounts and is connected by flexible seals to the tunnel on either side. The air speed does not change as the air passes through the fan, but there is an abrupt, stepwise increase in the static pressure. The rotational speed of the fan is controlled by a variable-frequency, solid-state power supply, also supplied by ABB.

Main diffuser, heat exchanger and large corners

The longest section on the lower level is the main diffuser, which begins at the downstream side of the fan casing and ends at the third corner. The cross-section of this diffuser diverges at a cone angle of 5 °, so that the velocity progressively decreases and the pressure rises. This effectively recovers the kinetic energy of the air by converting it into pressure energy. If the diffuser angle were wider than 5 °, the flow would be liable to separate from the walls, and this energy recovery would not take place. The heat exchanger is placed at the downstream end of the main diffuser and is connected to a cooler outside the tunnel. The two large corners take the air back to the upper level and restore the original flow direction.

Wide-angle diffuser, settling section and contraction

The final expansion after the second corner takes place in the wide-angle diffuser, at an angle of 18 °. Two wire-mesh screens force the flow to diverge at this wide angle. This leads to little further increase of pressure, but the energy loss is not great, as not much kinetic energy is left in the air by this stage. It was more practical to accept this energy cost than to complete the expansion to the entrance of the settling section at 5 °, which would have needed a longer machine and a bigger building to contain it. The settling section is the widest part of the tunnel, with a cross-sectional area of 13.7 m^2. A metal honeycomb at its entrance serves to align the air flow with the tunnel axis. This is followed by five fine wire-mesh screens, stretched across the settling section. Finally, the contraction accelerates the air by a factor of 12.25, reducing the pressure back to ambient atmospheric pressure at the entrance to the test section.

Structure

The structural backbone of the wind tunnel is the main diffuser, which is made of welded steel and is supported by the

tilt bearings between two steel tripods fixed to the concrete floor. A steel yoke at the wide end carries the nut that runs on the tilting screw. This is turned by an electric motor, operated remotely from the control position beside the test section. Also made of steel are the four casings for the corner vanes and the settling section casing. The screens are mounted in steel frames, which slide sideways into the settling section casing and can be removed for cleaning. The remaining tunnel sections are made of a plastic sandwich construction, with inner and outer fibreglass skins and plastic foam in between. This gives an extremely strong and rigid, but relatively light, structure with a smooth and accurate internal finish. The internal surfaces are finished black, to give a dark background for photography and also to discourage birds from venturing inside. The closed part of the test section is made from a welded aluminium frame, with removable acrylic panels. Only non-magnetic materials were used in this area, with the idea that the magnetic field in the test section might later be manipulated for orientation experiments.

Housing

The tunnel is 21 m long overall, stands 8 m above the floor and is 4.2 m wide. It is housed in a specially constructed building which has a gallery at the upper level to give access to the test section. A side extension at this level contains an environmentally controlled room providing work space and facilities for experimenters.

Instrumentation
Data monitoring system

In the hope of introducing some degree of uniformity into the way in which users of the wind tunnel record their data, we installed a system to measure and display a number of variables that are normally required for all experiments. Various sensors are read approximately once per second under the control of a Commodore Amiga 3000T computer, from which the current values of variables are calculated and continuously displayed on a monitor adjacent to the test section. The current data can also be printed out, either at regular intervals or on demand. The following variables are displayed: dynamic pressure and equivalent wind speed, barometric pressure, air temperature, air density, tilt angle and glide ratio.

Dynamic pressure and equivalent wind speed

Every wind tunnel must have some means of measuring the wind speed, but care is needed in distinguishing between different kinds of 'speed'. The primary variable that we monitor is actually the dynamic pressure (q), not the wind speed as such. This is defined as the pressure measured in a blind tube with the open end pointing into the wind, minus the static pressure. It is related to the true wind speed V thus:

$$q = \rho V^2/2, \qquad (1)$$

where ρ is the air density. The dynamic pressure is obtained from a differential pressure transducer (Setra 239: nominal precision

0.3 Pa), connected between two holes in the wall of the contraction, one at the wide end and one near the outlet. This pressure is proportional to, but less than, the dynamic pressure. It is converted into dynamic pressure by a linear calibration equation, which was obtained by measuring the actual dynamic pressure with a pitot-static probe in the test section connected to a manometer (Airflow Developments, type 4).

The *true* wind speed is the speed at which a light particle would be carried along, but we display and record the *equivalent* wind speed (V_e), to the nearest $0.1\,\mathrm{m\,s^{-1}}$. This is defined as:

$$V_e = \sqrt{(2q/\rho_0)}, \qquad (2)$$

where ρ_0 is the value assumed for the air density at sea level in the International Standard Atmosphere ($1.225\,\mathrm{kg\,m^{-3}}$). The true and equivalent wind speeds are the same only if the value of the air density actually is ρ_0. Otherwise, an experimenter wishing to test a bird under constant conditions does better to set a constant equivalent wind speed, rather than a constant true wind speed. This is because the equivalent wind speed is really an alternative way of expressing the dynamic pressure, and it is the dynamic pressure, not the speed as such, that determines the magnitudes of the forces on the wings and body. As the air density varies from day to day, owing to changes in barometric pressure and air temperature, a bird's characteristic speeds, such as the minimum power speed, remain more nearly constant in terms of equivalent than of true air speed.

Barometric pressure, air temperature and air density

Barometric pressure is obtained from an electrical pressure transducer (Setra 270) adjacent to the test section and is displayed to the nearest hPa. Air temperature is measured from a transducer embedded in the wall of the contraction and is displayed to the nearest $0.1\,°C$. From these, the air density (ρ) is calculated and is displayed to the nearest $0.01\,\mathrm{kg\,m^{-3}}$. The conversion factor between true and equivalent air speed is displayed as '$\sqrt{\sigma}$', where $\sigma = \rho/\rho_0$. This allows the true air speed to be easily calculated, should it be needed.

Tilt angle and glide ratio

A 10-bit digital shaft encoder geared to one of the main tilt bearings monitors the tilt angle in steps of $0.039\,°$ (2.3 arc min). The decoded output is displayed in degrees (positive for descent, negative for climb) and also as the glide ratio, defined as the cotangent of the tilt angle.

Performance
Wind speed and power

In initial tests, an equivalent wind speed of $37.6\,\mathrm{m\,s^{-1}}$ was obtained when the supply frequency to the motor was 50 Hz. The fan speed was 961 revs min^{-1} at 50 Hz, as against a nominal 980 revs min^{-1} at this supply frequency, and the measured power supplied to the motor was 26.7 kW, which is 72 % of its rated power (37 kW). The power factor for the
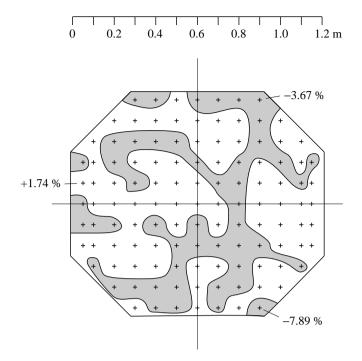
Fig. 3. Survey of equivalent wind speed in the wind tunnel, using a pitot-static probe placed at 119 points (crosses) in plane 4 (see Fig. 5). The wind speed was below the mean (21.28 m s^{-1}) at all points in the shaded area and above the mean at the points in the white area. The positions of three points where the wind speed deviated from the mean by anomalously large amounts are indicated. Speeds at the other 116 points deviated by less than 1.3 % from the mean.
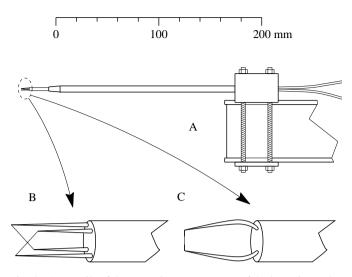

Fig. 4. (A) Details of the mounting arrangement of the hot-wire probe. The hot-wire probe was aligned with the flow direction, with the sensor tip upwind. (B,C) The two types of probe used. (B) Enlarged diagram of the X-wire probe (Dantec 55P61), showing 5 μm diameter sensor wires spot-welded to the tips of tapered metal prongs. (C) Enlarged diagram of the Dantec 55P01 probe, with a single 5 μm diameter sensor wire, copper- and gold-plated at each end.

tunnel, defined as the ratio of the observed electrical power to the kinetic energy flux in the test section, was 0.73. As the motor is rated for operation at frequencies up to 60 Hz, wind speeds up to 45 m s^{-1} should be obtainable if needed. The wind speed could be controlled smoothly by varying the supply frequency, and maintained steadily at any speed from zero up to the maximum. No resonances or wind speed fluctuations were observed.

Wind speed distribution in the test section

Fig. 3 shows the results of a survey carried out with a pitot-static probe at 119 points across the test section, on a 10 cm grid with some extra points at the sides. The tip of the probe was 14 cm upstream of the end of the closed part of the test section, in the plane marked P4 in Fig. 5. The motor speed was constant, giving a mean equivalent air speed of 21.28 m s^{-1}. Two points, in extreme corners on the right-hand side, showed wind speeds 3.7 % and 7.9 % below the mean, presumably because of thickening of the boundary layer in these corners, and a third point on the left side, also near the wall, showed an anomalous increase of 1.7 % over the mean. The speed at the remaining 116 points deviated by small amounts up to 1.3 % above or below the mean, with no 'hot spots' or 'dead spots' away from the walls. The standard deviation of speed, excluding the two 'retarded' points at the extreme top and bottom right, was 0.13 m s^{-1} or 0.59 % of the mean.

Hot-wire anemometer measurements

Turbulence levels and flow direction were investigated with a hot-wire anemometer system (Bruun, 1995) consisting of a Dantec 'Streamline' 90N10 frame, fitted with two 90C10 constant-temperature anemometry (CTA) modules and one 90H10 calibration module, which controlled a 90H02 flow unit for calibrating probes. One or both CTA modules were used, depending on whether the hot-wire probe in use had one or two wires. Each CTA module controlled one wire and consisted of a resistance bridge with circuitry that continuously adjusted the voltage across the wire, so as to hold its resistance (and hence its temperature) constant. The voltage required to do this serves as a measure of the rate at which heat is being carried away from the wire by the air stream and, hence, of the wind speed. Because of the small size and low thermal inertia of the wires, the system can follow variations of wind speed at frequencies up to several kilohertz. The analogue output of each CTA module was digitised by a Keithley Metrabyte DAS-1602 12-bit analogue-to-digital (A-D) converter, capable of digitising 10^5 samples s^{-1}. Dantec's 'Streamware' software (V1.10), running on a Hewlett Packard Vectra 486/25 VL computer, controlled all aspects of the calibration of the probes, setting up of the CTA modules, and capture and conversion of samples of digitised measurements from the A-D converter.

Two types of probes were used (Fig. 4). The Dantec 55P01 probe (Fig. 4C) had a single platinum-plated tungsten wire 5 μm in diameter, with copper and gold plating at the ends, isolating the active portion of the wire which was 1.25 mm long. The Dantec 55P61 probe (Fig. 4B) was an 'X-wire' type, in which two platinum-plated tungsten wires of 5 μm diameter were inclined at 45 ° to the air flow and at 90 ° to each other.
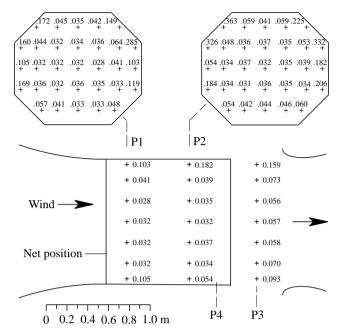
Fig. 5. Cross sections of the test section, showing turbulence measurements at 31 points in each of survey planes 1 and 2 (P1, P2). The overhead view shows the location of each survey plane, with the measurements in the centre horizontal row. These are also shown for plane 3, in the middle of the open part of the test section. The numbers represent root mean square (RMS) wind speed fluctuations, expressed as a percentage of the mean wind speed. Plane 4 is the location of the pitot-static survey (see Fig. 3) and also of the wall-effect traverse (see Fig. 8).

This type of probe gives two independent measurements, which can be used for measuring flow velocities in two dimensions. The mounting arrangement of the hot-wire probe is shown in Fig. 4A. The ceramic stem of the probe was supported by a straight holder 235 mm long, inserted into an aluminium alloy block and aligned with the air flow. The block was clamped to the end of a 60 mm deep aluminium I-beam (actually a spirit level 1200 mm long), and the beam in turn was clamped to the head of a heavy photographic tripod. The tripod stood in the open part of the test section on a board which could be used as a hand-operated traversing system, by sliding it transversely to the tunnel axis, against a guide rail bearing a scale.

Turbulence level in the test section

The 55P01 single-wire probe was used to survey planes 1 and 2 in the closed part of the test section, 20 and 80 cm respectively downstream of the entrance (Fig. 5), and also the centre horizontal row of points in plane 3, in the middle of the open part. Two samples, each consisting of 1024 observations of wind speed, were taken at a sampling frequency of 1 kHz at each of the 69 points shown in Fig. 5. As no anomalies were found in the 'repeat' samples, each pair of samples was later combined into a single sample. The values in Fig. 5 represent the standard deviation of the air speed in each sample, expressed as a percentage of the wind speed. This is the same
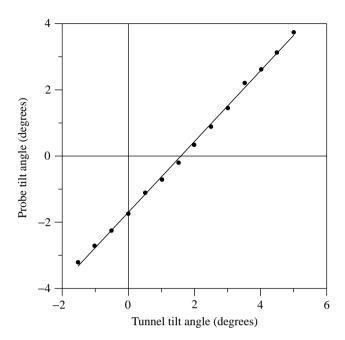

Fig. 6. Linear regression of tilt angle, as measured by the X-wire probe (see Fig. 4B), *versus* the actual tilt angle of the tunnel (*r*=0.999). The slope (1.07) is as close to 1 as could be expected, given the limitations of the angular calibration procedure, and likewise the offset. Equivalent air speed was 10 m s^{-1}.

as the RMS fluctuation, conventionally used by wind tunnel engineers as a measure of the level of turbulence. Fig. 5 shows that the turbulence level was below 0.04 % throughout most of the closed part of the test section, rising to approximately 0.06 % in the middle of the open part (plane 3). We noticed that small amounts of vibration affecting the probe caused an increase in the measured turbulence level, and also that the turbulence increased for some minutes following a change in the wind speed. After the tunnel had been standing overnight, we had to run it for at least 30 min to allow mixing of air which had equilibrated at different temperatures in different parts of the circuit. Despite all precautions, it is difficult to be sure that no such artefacts biased our results upwards, and the true levels of turbulence in the air stream could have been even lower than the recorded values. Although the turbulence levels shown in Fig. 5 are very low, they should be regarded as 'upper bounds'.

Flow direction and the effect of a net

We used the 55P61 X-wire probe to survey the turbulence level in plane 2, after installing a net, made of braided nylon cord, 0.75 mm in diameter, with a square mesh 17 mm×17 mm, at the upstream end of the test section. This net was used during training to prevent birds from flying into the contraction and also during wingbeat frequency measurements on a teal (*Anas crecca*) reported by Pennycuick *et al.* (1996). The turbulence level with the net installed averaged 1.21 % parallel to the flow direction, more than 30 times higher than that observed without the net. The turbulence level transverse to the flow direction was slightly lower, at 1.03 %.
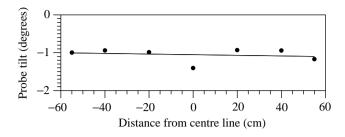
Fig. 7. Tilt angle, as measured by the X-wire probe (see Fig. 4B), across the centre line of plane 2 (see Fig. 5), with the tunnel horizontal (r=−0.192). Equivalent air speed was $10\,\mathrm{m\,s^{-1}}$.

Calibration of the probe for two-dimensional measurements depends on hand-setting of the probe holder in the flow unit, using a small scale marked in intervals of 5°. We checked this angular calibration by positioning the probe near the middle of plane 2, then tilting the tunnel from −1.52° (bird climbing) to +5.00° (bird descending), while the probe remained horizontal (Fig. 6). Finally, we removed the net and re-surveyed the horizontal centre line of plane 2 with the tunnel horizontal, using the 55P61 probe to see whether any residual rotation from the fan remained. The apparent flow direction varied within a 0.5° range, but showed no sign of residual rotation (Fig. 7). The offset in Fig. 7 was due to the limited precision of the angular calibration.

Flow near the walls

We used the 55P01 probe to observe the influence of the walls on the flow. For this test, the probe was positioned 15 cm above the centre line and was moved from the centre of the test section to 1 cm from the left wall, in diminishing steps as shown in

Fig. 8. Wind speed (open circles) and turbulence level (filled circles) measured in plane 4 (see Fig. 5) with the single-wire probe (see Fig. 4C), at seven positions from the centre line to 1 cm from the left wall (see inset). Equivalent air speed was $10\,\mathrm{m\,s^{-1}}$.
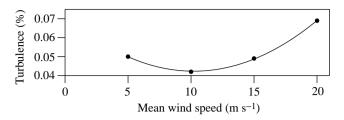

Fig. 9. Turbulence level at different wind speeds, with the probe at the centre point of plane 2 (see Fig. 5). The fitted curve is a second-degree polynomial.

Fig. 8. The probe tip was 14 cm upstream of the exit from the closed part of the test section. Fig. 8 shows that the turbulence level, even at this downstream location, was very low to within 10 cm of the wall, while the wind speed was effectively constant to within 3 cm of the wall. We recommend that the wing span of birds flying in the tunnel should not exceed two-thirds of the width of the test section (80 cm), so as to remain in the best quality air flow, and also to minimise the effect of the walls on the flow around the wings, as mentioned above.

Variation of turbulence with wind speed

With the 55P01 probe in a fixed position, at the centre point of plane 2, we measured the turbulence level at four different wind speeds, from 5 to $20\,\mathrm{m\,s^{-1}}$. The lowest turbulence was at $10\,\mathrm{m\,s^{-1}}$ (Fig. 9).

References

BARRETT, R. V. (1984). Design and performance of a new low turbulence wind tunnel at Bristol University. *Aeronaut. J.* **88**, 86–90.

BRUUN, H. H. (1995). *Hot-wire Anemometry: Principles and Signal Analysis*. Oxford: Oxford University Press.

GREENEWALT, C. H. (1961). *Hummingbirds*. New York: Doubleday.

NACHTIGALL, W. (1995). Impositions on energy balance in prolonged flight: wind tunnel measurements with 'model birds'. *Israel J. Zool.* **41**, 279–295.

PANKHURST, R. C. AND HOLDER, D. W. (1965). *wind tunnel Technique* (2nd edition). London: Pitman.

PENNYCUICK, C. J. (1968). A wind tunnel study of gliding flight in the pigeon *Columba livia*. *J. exp. Biol.* **49**, 509–526.

PENNYCUICK, C. J., KLAASSEN, M., KVIST, A. AND LINDSTRÖM, Å. (1996). Wingbeat frequency and the body drag anomaly: wind tunnel observations on a thrush nightingale (*Luscinia luscinia*) and a teal (*Anas crecca*). *J. exp. Biol.* **199**, 2757–2765.

RAE, W. H. AND POPE, A. (1984). *Low-speed Wind Tunnel Testing* (2nd edition). New York: Wiley.

ROSÉN, J. AND NYSTRÖM, T. (1997). The low speed tiltable wind tunnel SWT112. *Proceedings of the 20th Congress of the International Council of Aeronautical Sciences* (in press).

ROTHE, H.-J. AND NACHTIGALL, W. (1987). Pigeon flight in a wind tunnel. *J. comp. Physiol.* B **157**, 91–98.

SCHMITZ, F. W. (1960). *Aerodynamik des Flugmodells* (4th edition). Duisberg: Lange.

SIMONS, M. (1994). *Model Aircraft Aerodynamics* (3rd edition). Hemel Hempstead: Argus.

TUCKER, V. A. AND PARROTT, G. C. (1970). Aerodynamics of gliding flight in a falcon and other birds. *J. exp. Biol.* **52**, 345–367.